

Synchrotron and Inverse Compton Scattering Radiation from Galactic Dark Matter

Gennaro Miele

University of Naples “Federico II”



In collaboration with

E. Borriello - University of Naples “Federico II”

A. Cuoco - University of Aarhus – DK

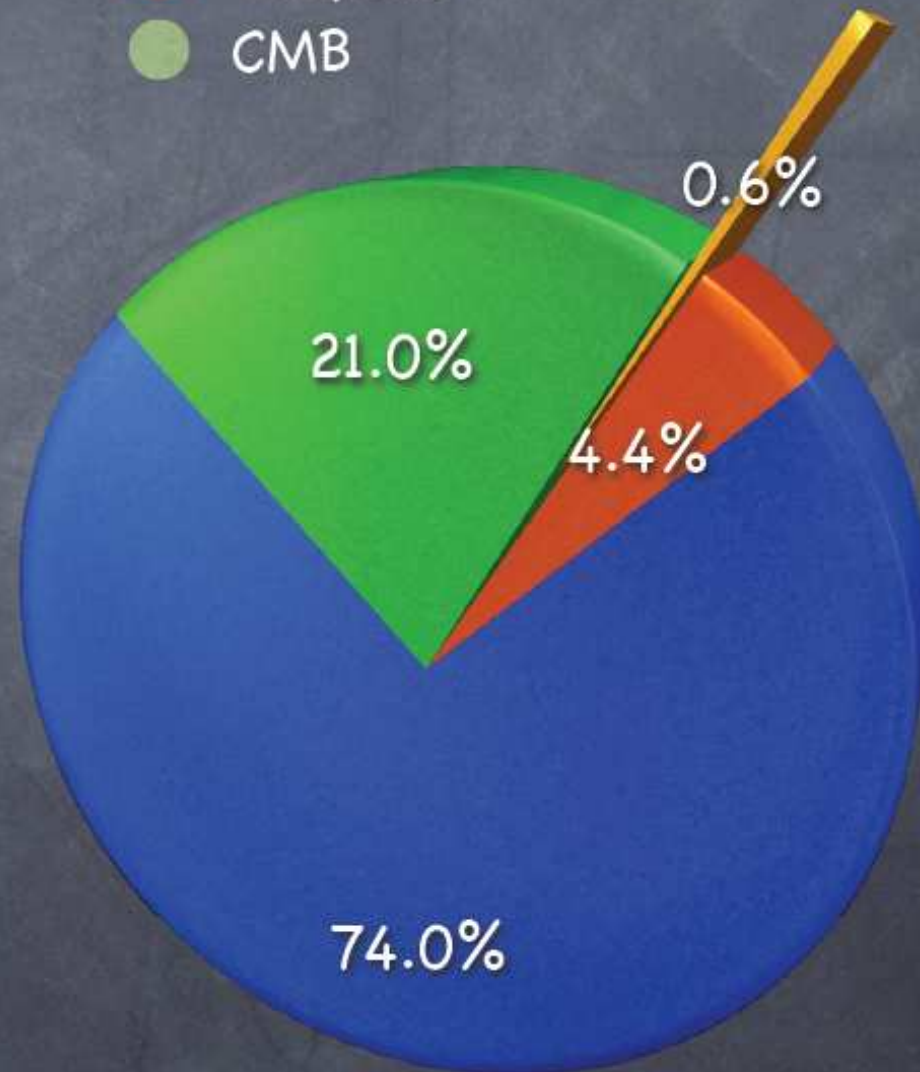
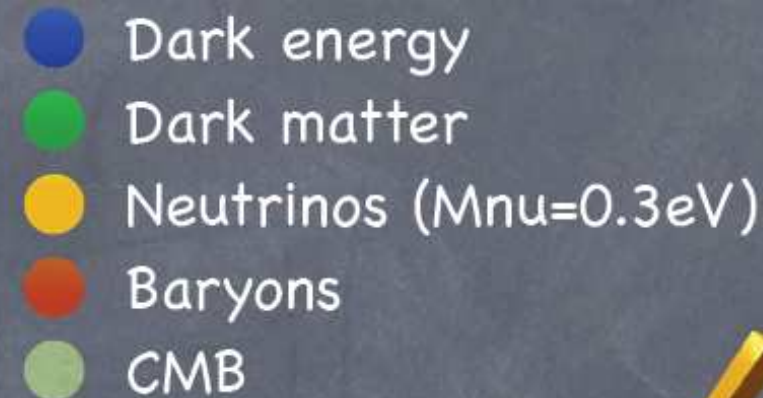
Based on

- PRD 79, 023518 (2009)
- 0903.1852 [astro-ph.GA]



Motivations

- Cosmology and Astrophysics provide a striking evidence for **DM**
- Promising candidates for **DM** particles are the so-called **WIMP**
- **WIMPs** are realized in SUSY as the Lightest Super-symmetric Particle (**LSP**) or as the Lightest Kaluka-Klein Particle (**LKP**)

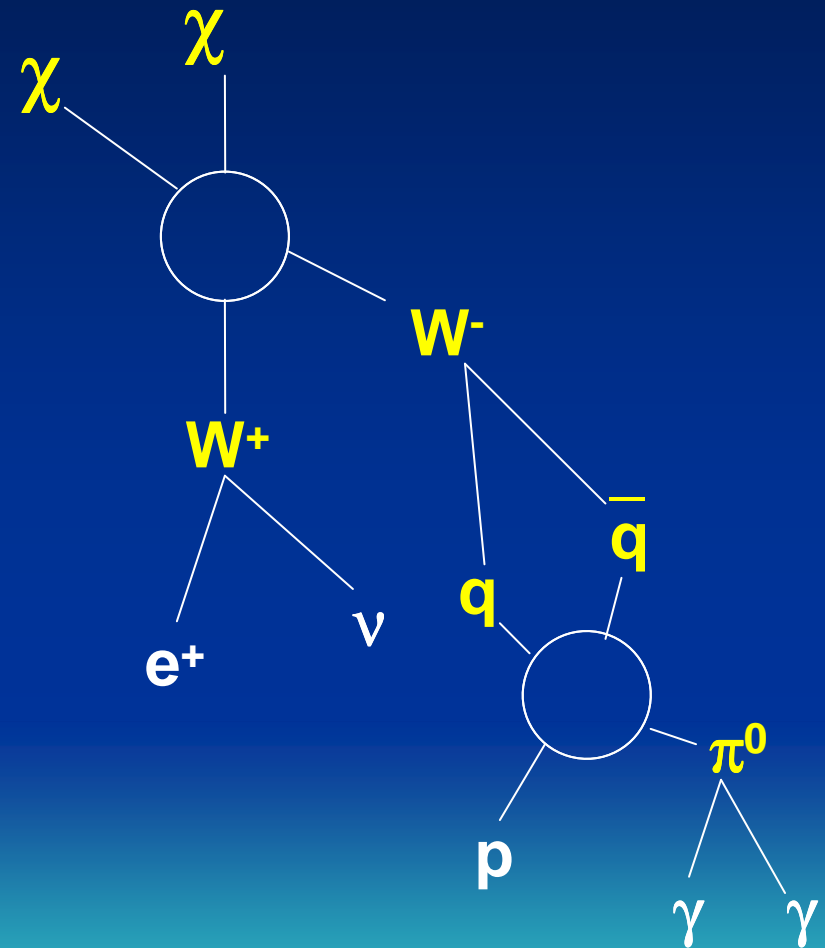


➤ These candidates are self-conjugate thus annihilating in couple produce as final states neutrinos, photons, electrons, light nuclei (as well as their antiparticles) (**Indirect DM detection!**).

✓ e^+e^- once in the galactic environment, interact with the **Galactic Magnetic Field** (GMF) and the **InterStellar Radiation Field** (ISRF).

✓ They will lose energy producing **Synchrotron Radiation** (SR) in the radio band and **Inverse Compton Scattering** (ICS) Radiation in the gamma band.

✓ **Need for a Multiwavelength Approach**

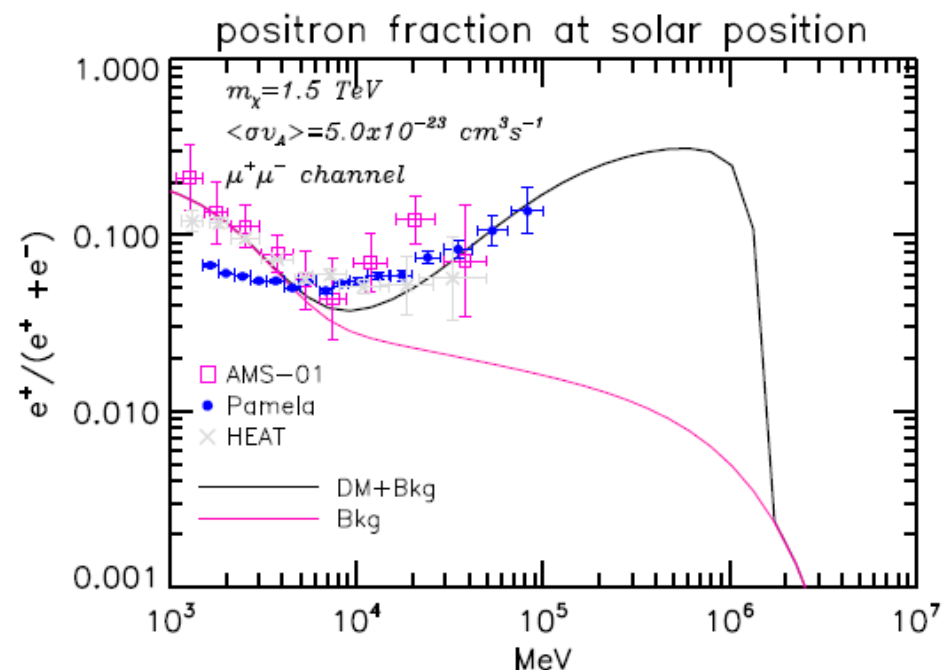
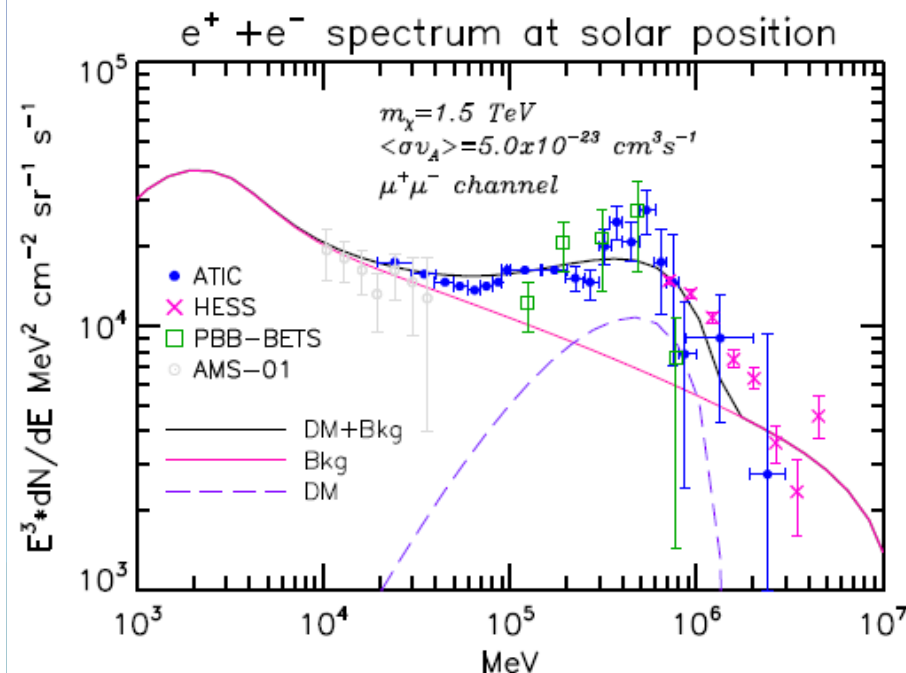


Pamela & ATIC results

ATIC – An excess of $e^+ + e^-$ between ~ 100 GeV and ~ 700 GeV

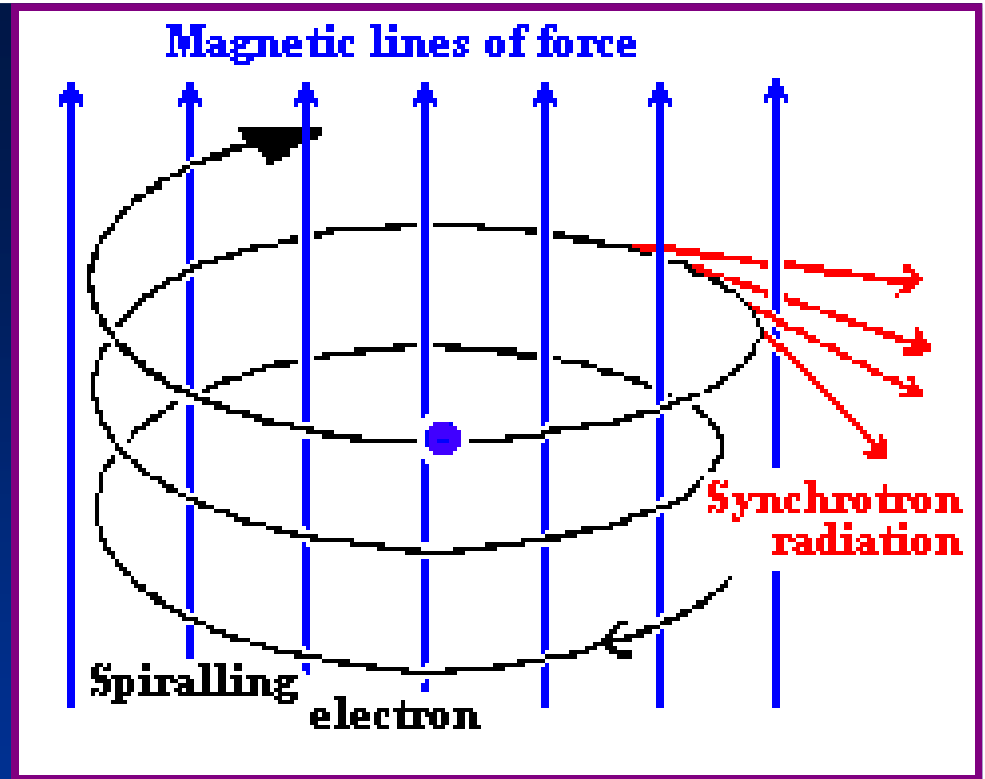
Pamela – A raise in the positron fraction above 10 GeV until ~ 100 GeV

Require a new source of electrons/positrons





➤ Charged leptons and nuclei strongly interact with gas, radiation and Galactic Magnetic Field. During the process of thermalization $HE\ e^+e^-$ release secondary low energy radiation, in particular in the radio and X-ray band (in principle detectable).



Due to Inverse Compton Scattering on starlight and CMB and Synchrotron on galactic Magnetic Field one gets

$$-\frac{1}{E_e} \left(\frac{dE_e}{dt} \right) = \left(\frac{1}{\tau_{syn}} + \frac{1}{\tau_{ICS}} \right)$$

The two energy loss time scales are

$$\tau_{syn} \cong 4 \cdot 10^{17} \left(\frac{B}{\mu G} \right)^{-2} \left(\frac{E_e}{GeV} \right)^{-1} \text{ sec}$$

$$\tau_{ICS} \cong 10^{16} \left(\frac{U_{rad}}{eV / cm^3} \right)^{-1} \left(\frac{E_e}{GeV} \right)^{-1} \text{ sec}$$

- While the astrophysical uncertainties affecting this signal are similar to the case of direct e^+e^- detection, the sensitivities are quite different and, in particular in the radio band, allows the discrimination of tiny signals even with backgrounds many order of magnitudes more intense.
- Interestingly, for Electroweak-Scale DM, the resulting synchrotron radiation falls within the frequency range of WMAP.

Model outline

- **ASTROPHYSICAL INPUTS**
 - Dark Matter Distribution
 - Galactic Magnetic Field
 - Radio Data
- **DM SYNCHROTRON SIGNAL**
 - Particle Physics
 - Electrons equilibrium distribution
 - Synchrotron spectrum
- **DM ANNIHILATION CONSTRAINTS**

Dark Matter Distribution

Our knowledge of the DM spatial distribution on galactic and subgalactic scales has greatly improved thanks to recent high resolution zoomed N-body simulations. The galactic halo seems very well described by the Navarro-Frank-White (NFW) distribution (conservative point of view)

$$\rho(r) = \frac{\rho_h}{\frac{r}{r_h} \left(1 + \frac{r}{r_h} \right)^2}$$

Beside the smooth halo component DM is also distributed into a clumpy component with the two total masses \sim of the same order of magnitude

Concerning clumps their mass range from $10^{-6} M_{\odot}$ up to $10^{10} M_{\odot}$. However $10^7 M_{\odot}$ represents the minimum scale which actual numerical simulations can resolve.

We will assume an universal NFW profile for the mass spectrum number density of subhaloes, in galactocentric coordinates

$$\frac{dn_{\text{cl}}}{dm_{\text{cl}}}(m_{\text{cl}}, \vec{r}) = A \left(\frac{m_{\text{cl}}}{M_{\text{cl}}} \right)^{-2} \left(\frac{r}{r_h} \right)^{-1} \left(1 + \frac{r}{r_h} \right)^{-2}$$

$$\begin{aligned} M(m_1, m_2) &= \int d\vec{r} \int_{m_1}^{m_2} m_{\text{cl}} \frac{dn_{\text{cl}}}{dm_{\text{cl}}}(m_{\text{cl}}, \vec{r}) dm_{\text{cl}} \\ &= 4\pi \left[\ln(1 + c_h) - \frac{c_h}{1 + c_h} \right] (A r_h^3 M_{\text{cl}}) \\ &\quad \times \ln \left(\frac{m_2}{m_1} \right) M_{\text{cl}} , \end{aligned}$$

$C_h = r_h/r_{\text{vir}}$ is the halo concentration

$$\begin{aligned} N(m_1, m_2) &= \int d\vec{r} \int_{m_1}^{m_2} \frac{dn_{\text{cl}}}{dm_{\text{cl}}}(m_{\text{cl}}, \vec{r}) dm_{\text{cl}} \\ &= 4\pi \left[\ln(1 + c_h) - \frac{c_h}{1 + c_h} \right] (A r_h^3 M_{\text{cl}}) \\ &\quad \times \left(\frac{M_{\text{cl}}}{m_1} - \frac{M_{\text{cl}}}{m_2} \right) . \end{aligned}$$



By fixing $M_{MW} = M_h + M_{cl} = 2 \times 10^{12} M_\odot$

And imposing that:

- the total mass in subhaloes between $10^7 M_\odot$ and $10^{10} M_\odot$ amounts to 10% of M_{MW} (simulations);
- the DM density near the Solar System, at a galactocentric distance of $R_S = 8.5 \text{ kpc}$, is equal to $\rho_S = 0.365 \text{ GeV cm}^{-3}$

One gets $M_{cl} \sim 53.3 \% M_{MW}$

$$N(10^{-6} M_\odot, 10^{10} M_\odot) \sim 2.9 \times 10^{17}$$

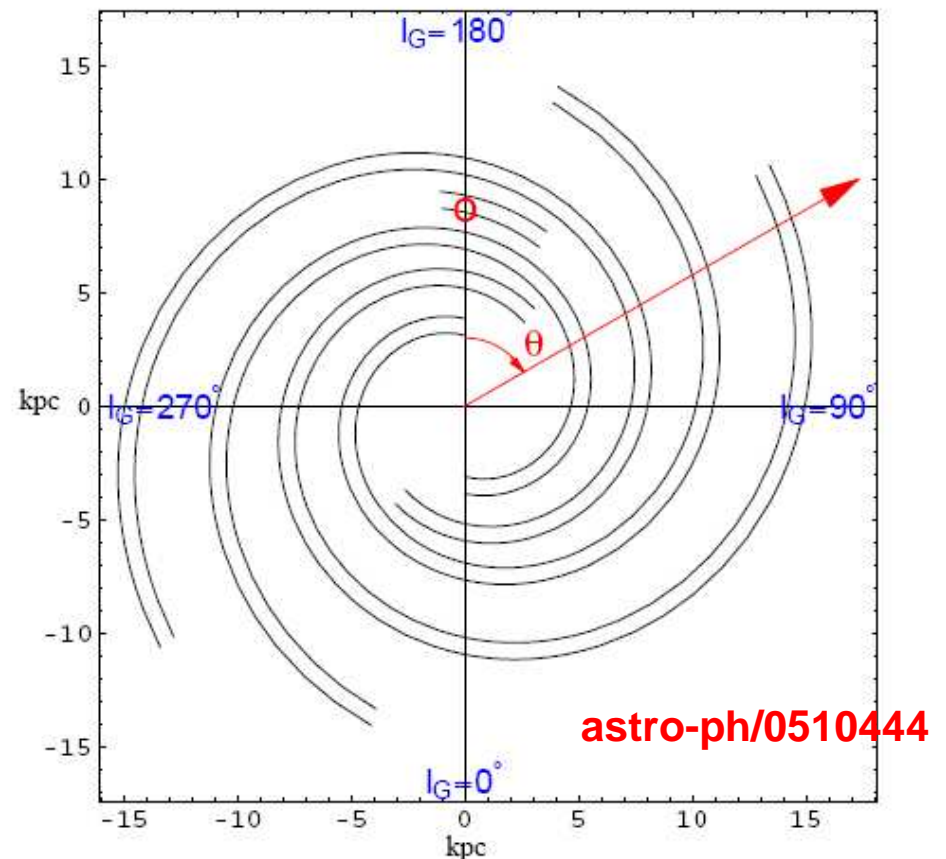
$r_h = 14.0 \text{ kpc}$, that corresponds to a halo concentration of $c_h = 14.4$, and $\rho_h = 0.572 \text{ GeV c}^{-2} \text{ cm}^{-3}$ and $A = 1.16 \cdot 10^{-19} \text{ kpc}^{-3} M_\odot^{-1}$

Even each clump is described by an internal NFW

Galactic Magnetic Field

The MW magnetic field is still quite uncertain especially near the galactic center. The overall structure is generally believed to follow the spiral pattern of the galaxy itself with a normalization of about $\sim 1 \mu\text{G}$ near the solar system. A toroidal or a dipole component is considered in some model.

We use a typical spiral pattern (Tinyakov and Tkachev model) with an exponential decreasing along the z axis and a $1/r$ behavior in the galactic plane. The field intensity in the inner kpc's is constant to about $7 \mu\text{G}$.



Radio Data

Constraints on the DM emission are obtained comparing the expected diffuse emission from the “smooth halo” and the unresolved population of “clumps” with all sky observation in the radio band. In the frequency range between 100 MHz-100 GHz where the DM synchrotron signal is expected

Competing synchrotron emission is given by

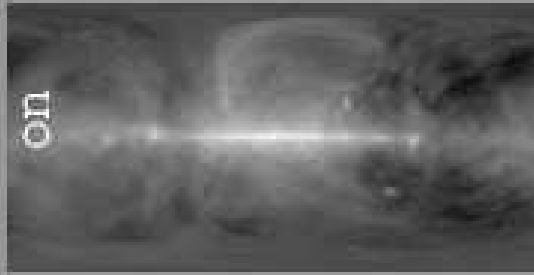
- Cosmic Ray electrons accelerated in supernovae shocks, dominate up to ~ 10 GHz.
- At higher frequencies CMB and its anisotropies represent the main signal.

Thanks to the very sensitive multi-frequency survey by the WMAP (22.8, 33.0, 40.7, 60.8 and 93.5 GHz), this signal can be modeled and thus removed from the observed radio galactic emission.

Other processes contributing in the 10-100 GHz range

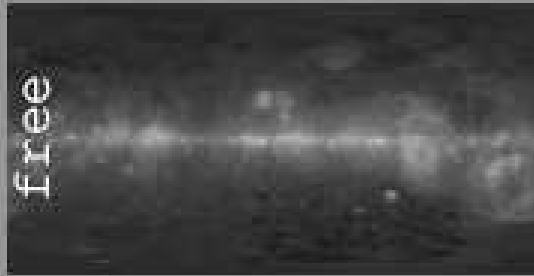
- Synchrotron Radiation (low energy)
- Thermal bremsstrahlung (free-free emission) of electrons on the galactic ionized gas (low energy)
- Emission by small grains of vibrating or spinning dust (high energy)

Synchrotron



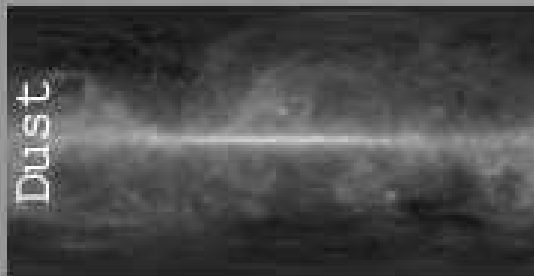
+

Free-free



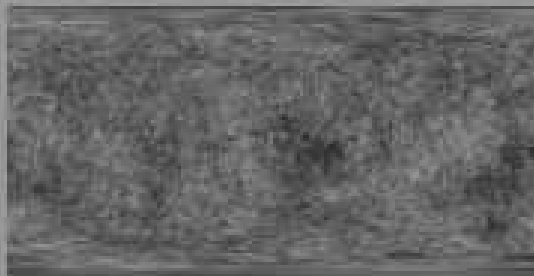
+

T & S
Dust

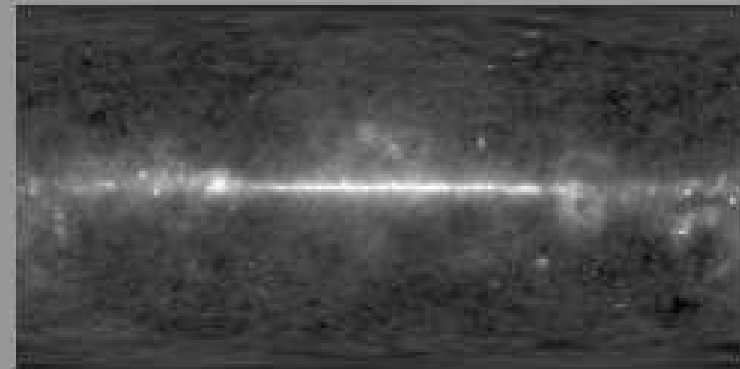


+

CMB



=

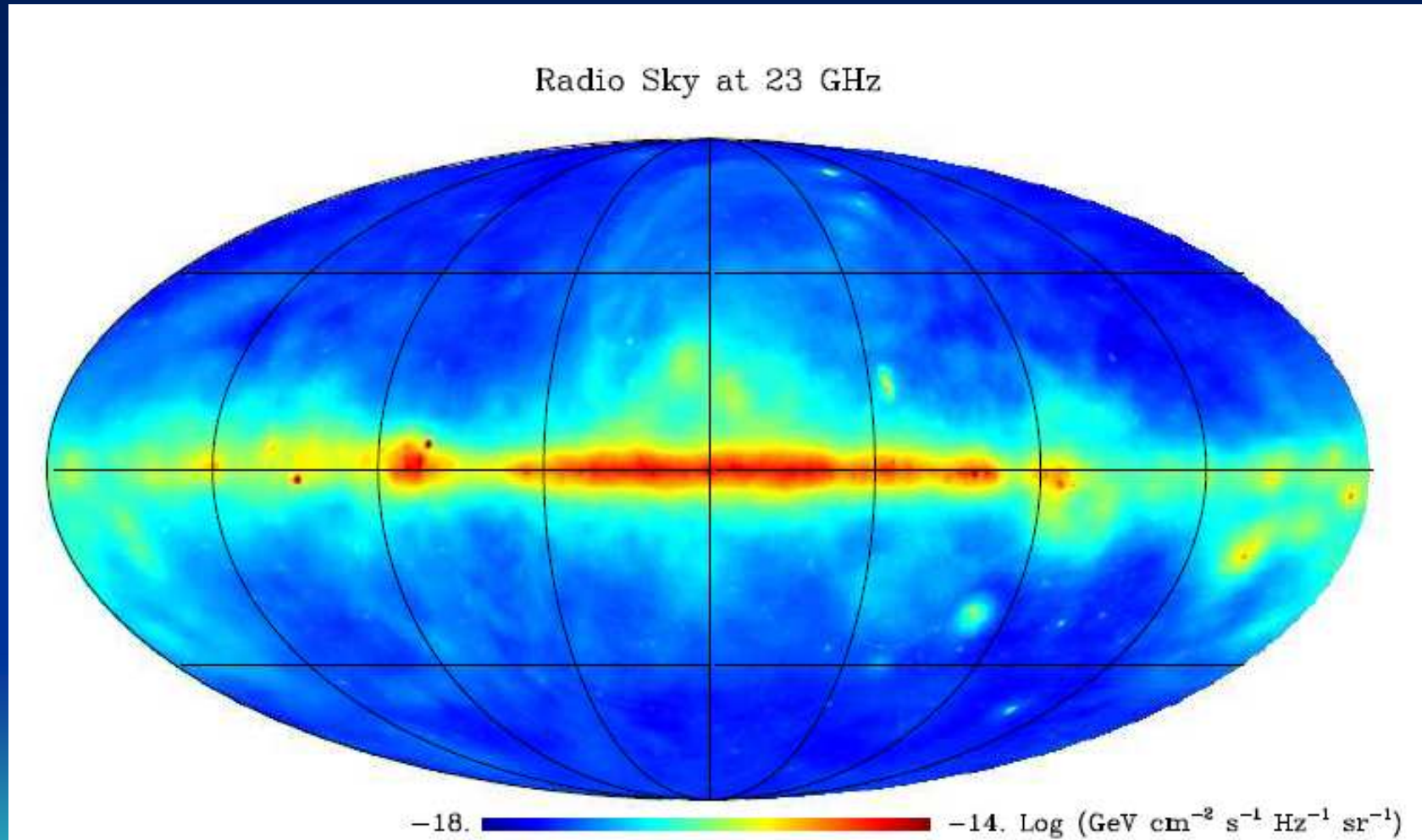


WMAP

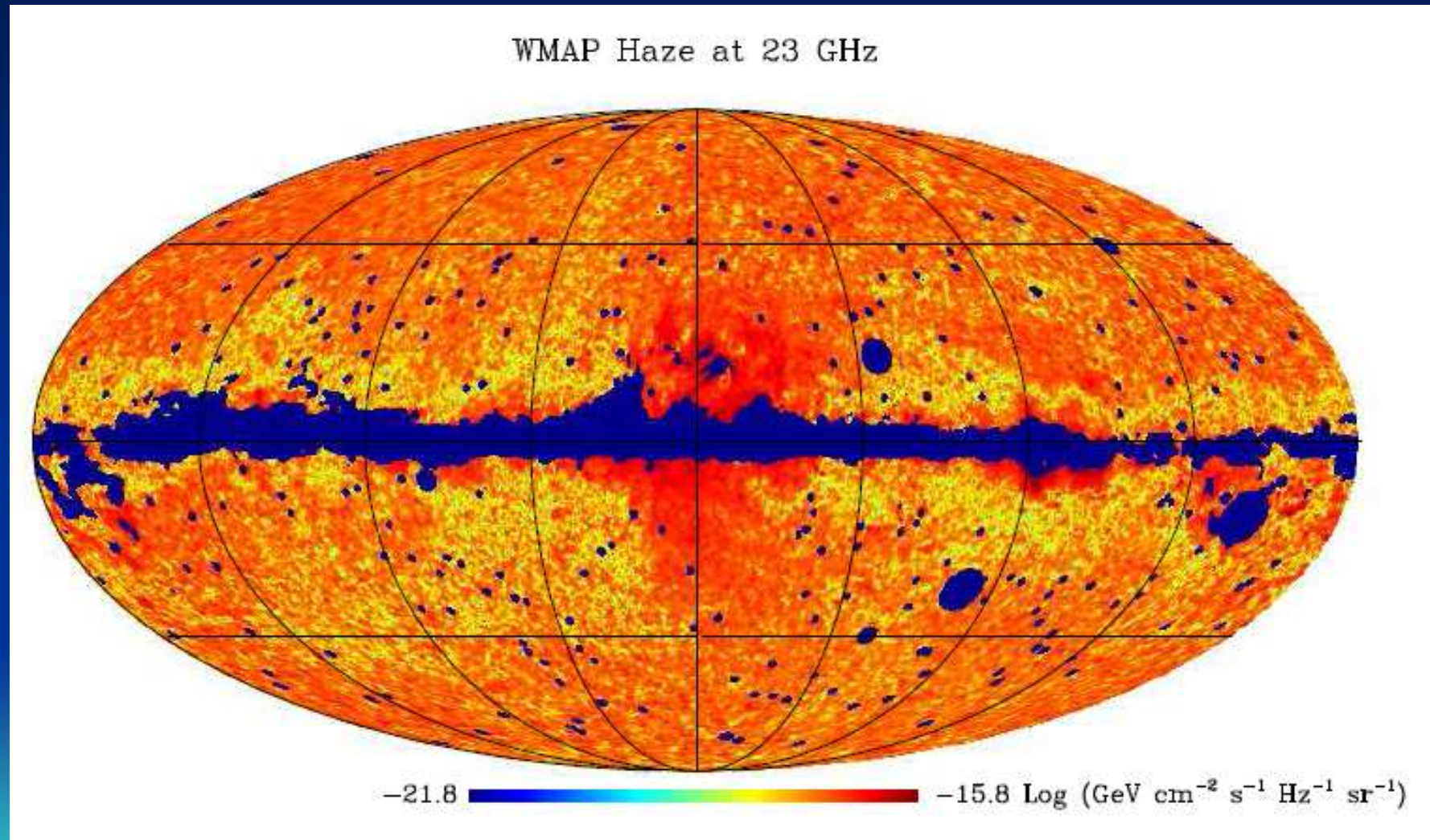
Well, actually... No

Dan Hooper - *Dark Matter Annihilations
in the WMAP Sky*

Sky map of galactic foregrounds at 23 GHz



Residual map showing the WMAP Haze at 23 GHz



Our approach:

To compare the DM signal with the observed radio emission where only the CMB is modeled and removed. For this purpose we have used the code described in [arXiv:0802.1525\[astro-ph\]](#) where most of the radio survey observations in the range 10 MHz - 100 GHz are collected and a scheme to derive interpolated, CMB cleaned sky maps at any frequency in this range is described.

We consider a χ mass range of $50 \text{ GeV} \lesssim m_\chi \lesssim 500 \text{ GeV}$ and $\langle \sigma_A v \rangle = (10^{-26} - 10^{-21}) \text{ cm}^3 \text{ s}^{-1}$

$$\chi + \chi \longrightarrow q + \bar{q} \longrightarrow \pi^\pm + X$$

**Neutralinos mainly
annihilate in the
hadronic channel**

$$\downarrow \nu_\mu + \mu^\pm$$

$$\downarrow \nu_e + \nu_\mu + e^\pm$$

$$\frac{dN_e}{dE_e}(E_e) = \int_{E_e}^{m_\chi c^2} dE_\mu \frac{dN_e^{(\mu)}}{dE_e}(E_e, E_\mu) \\ \times \int_{E_\mu}^{E_\mu/\xi} dE_\pi W_\pi(E_\pi) \frac{dN_\mu^{(\pi)}}{dE_\mu}(E_\pi)$$

with $\xi = (m_\mu/m_\pi)^2$, where

$$\frac{dN_e^{(\mu)}}{dE_e}(E_e, E_\mu) = \frac{2}{E_\mu} \left[\frac{5}{6} - \frac{3}{2} \left(\frac{E_e}{E_\mu} \right)^2 + \frac{2}{3} \left(\frac{E_e}{E_\mu} \right)^3 \right],$$

$$\frac{dN_\mu^{(\pi)}}{dE_\mu}(E_\pi) = \frac{1}{E_\pi} \frac{m_\pi^2}{m_\pi^2 - m_\mu^2},$$

$$W_\pi(E_\pi) = \frac{1}{m_\chi c^2} \frac{15}{16} \left(\frac{m_\chi c^2}{E_\pi} \right)^{\frac{3}{2}} \left(1 - \frac{E_\pi}{m_\chi c^2} \right)^2$$

Electron Equilibrium Distribution

Dark matter annihilation injects electrons in the galaxy at the constant rate

$$Q(E_e, r) = \frac{1}{2} \left(\frac{\rho(r)}{m_\chi} \right)^2 \langle \sigma_A v \rangle \frac{dN_e}{dE_e}$$

The injected electrons loose energy in the interstellar medium and diffuse away from the production site.

$$\begin{aligned} \frac{\partial}{\partial t} \frac{dn_e}{dE_e} = & \vec{\nabla} \cdot \left[K(E_e, \vec{r}) \vec{\nabla} \frac{dn_e}{dE_e} \right] + \frac{\partial}{\partial E_e} \left[b(E_e, \vec{r}) \frac{dn_e}{dE_e} \right] \\ & + Q(E_e, \vec{r}), \end{aligned}$$

The diffusion length of electrons is generally of the order of a kpc thus for the diffuse signal generated all over the galaxy, spatial diffusion can be safely neglected. This is not the case for the signal coming from a single clump for which the emitting region is much smaller than a kpc.

Neglecting spatial diffusion, steady state solution reads

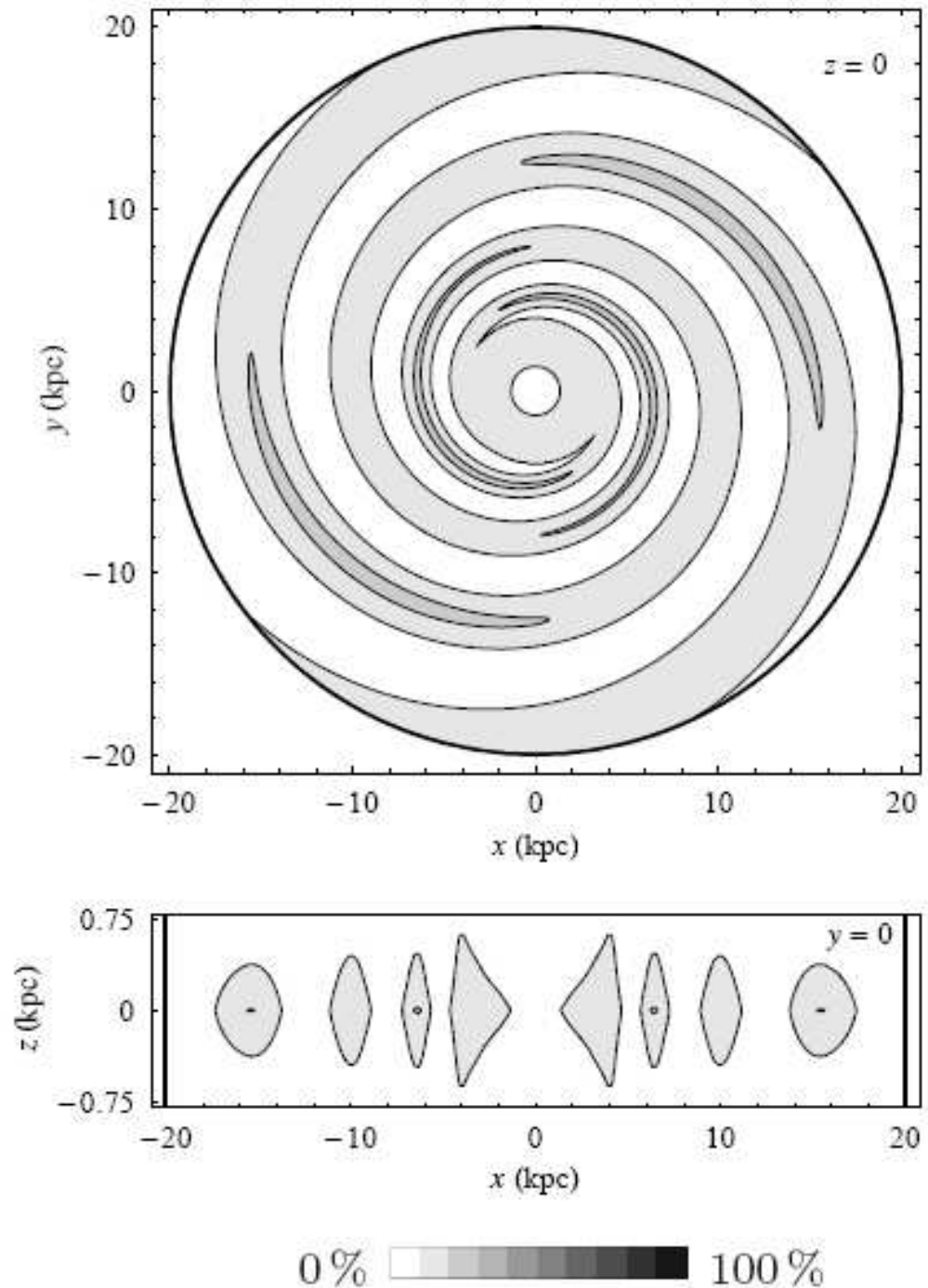
$$\frac{dn_e}{dE_e}(E_e, \vec{r}) = \frac{\tau}{E_e} \int_{E_e}^{m_\chi c^2} dE Q(E, \vec{r})$$

where τ is the cooling time resulting from the sum of several energy loss processes: Synchrotron emission and Inverse Compton Scattering (ICS) on the background photons (CMB and starlight) only $1/\tau = 1/\tau_{\text{syn}} + 1/\tau_{\text{ICS}}$

$$\tau(E_e, \vec{r}) = \left(\frac{E_e}{\text{GeV}} \right)^{-1} \mu(\vec{r}) 9.82 \cdot 10^{15} \text{ s}$$
$$\mu(\vec{r}) = \left[\left(\frac{B(\vec{r})}{\mu\text{G}} \right)^2 + 40.2 \frac{U_{\text{rad}}(\vec{r})}{\text{eV} / \text{cm}^3} \right]$$

Other processes, like synchrotron self absorption (ICS on the synchrotron photons), e^+e^- annihilation, Coulomb scattering over the galactic gas and bremsstrahlung are generally slower. They can become relevant for extremely intense MF.

Projections of the galaxy in the xy and xz planes showing the fractional synchrotron contribution to the e^\pm total energy losses for TT model of GMF and Galprop model of ISRF. The synchrotron losses contribute up most to 20% reaching its maximum at the center of the magnetic arms. In the remaining regions, included the galactic center, ICS is dominating.



Synchrotron spectrum

The synchrotron spectrum of an electron gyrating in a magnetic field has prominent peak at the resonance frequency

$$\nu = 3.7 \left(\frac{B}{\mu G} \right) \left(\frac{E_e}{GeV} \right)^2 \text{ MHz}$$

Using this *frequency peak* approximation, the *synchrotron emissivity* can be defined as

$$j_\nu(\nu, \vec{r}) = \frac{dn_e}{dE_e}(E_e(\nu), \vec{r}) \frac{dE_e(\nu)}{d\nu} \frac{E_e(\nu)}{\tau_{syn}}$$

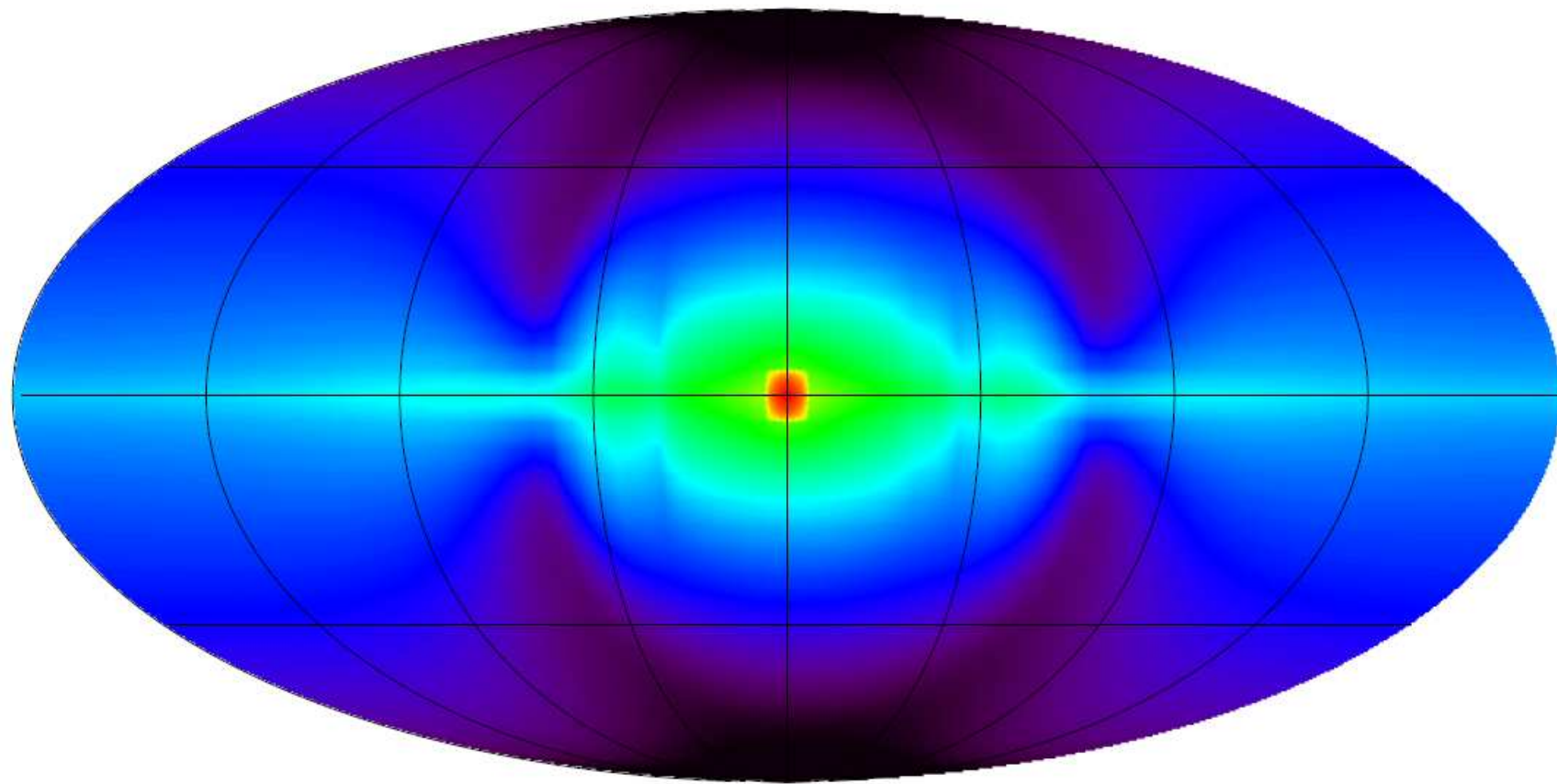
Summing the smooth halo and clump distribution terms one gets

$$j_{\nu}^{\text{DM}} = \frac{1}{4} \left(\frac{m_{\chi} c^2}{\text{GeV}} \right)^{-3} \frac{\langle \sigma_A v \rangle}{\text{cm}^3 \text{s}^{-1}} \left\{ \left[\frac{\rho_h / \text{GeV} c^{-2} \text{cm}^{-3}}{(r/r_h)(1 + r/r_h)^2} \right]^2 + \frac{\rho_{\text{CL}} / \text{GeV} c^{-2} \text{cm}^{-3}}{(r/r_h)(1 + r/r_h)^2} \right\} \\ \mu(\vec{r}) \sum_k A_k(m_{\chi}) \left(\frac{B(\vec{r})}{\mu\text{G}} \right)^{1-k/2} \left(\frac{\nu}{\text{Hz}} \right)^{k/2} \text{GeV cm}^{-3} \text{s}^{-1} \text{Hz}^{-1} \text{sr}^{-1} .$$

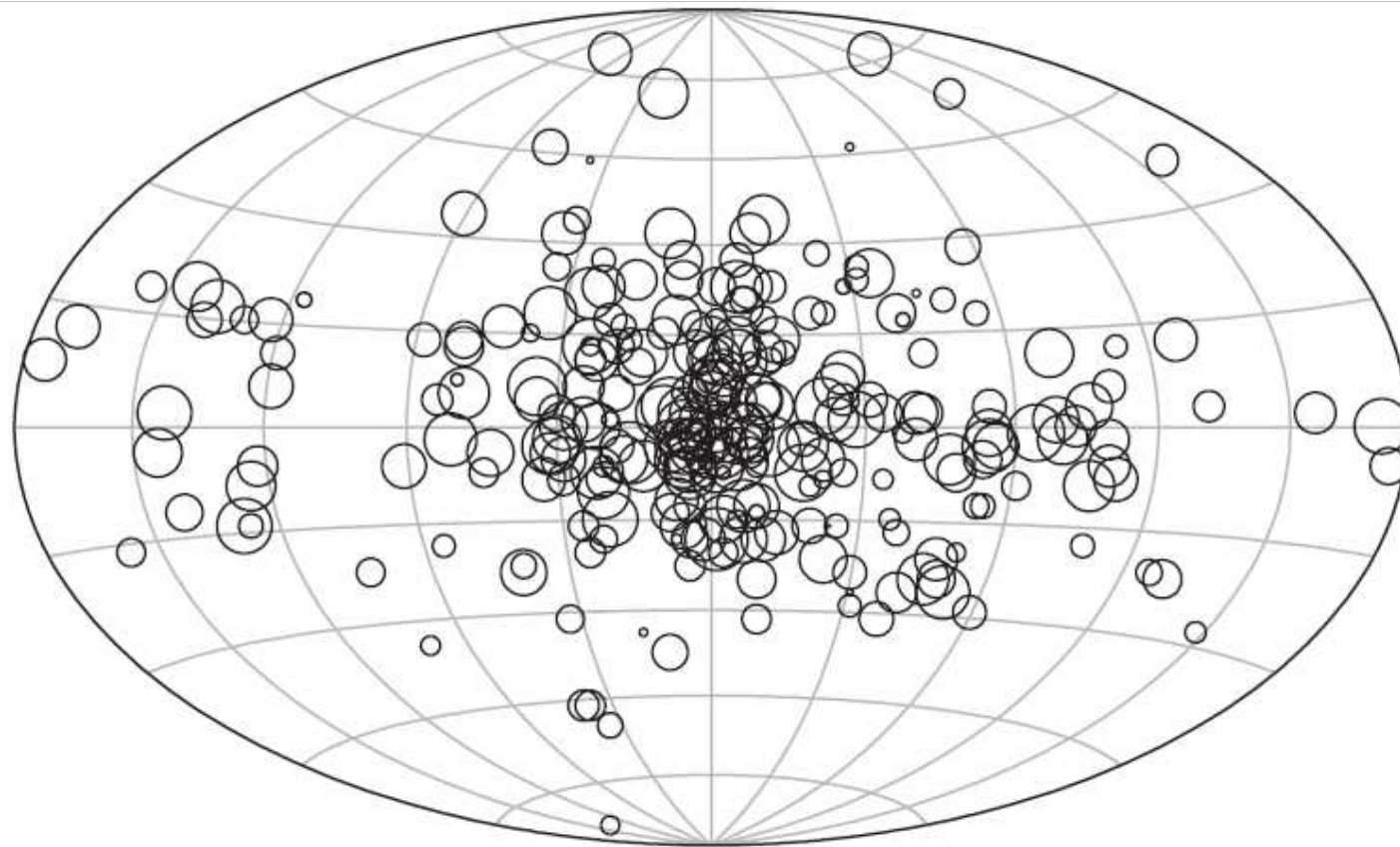
Interestingly, from the point of view of DM annihilation the unresolved clumps signal behaves like a further smooth NFW component with the same scale radius of the halo profile, but with a different *effective density*

Sky map of the galactic radio signal generated by the DM smooth halo at the frequency of 1 GHz.

DM synchrotron at 1 GHz



-21.1  -15.1 $\text{Log (GeV cm}^{-2} \text{ s}^{-1} \text{ Hz}^{-1} \text{ sr}^{-1}\text{)}$



flux density ($\text{GeV cm}^{-2} \text{s}^{-1} \text{Hz}^{-1}$)

\bigcirc 10^{-18}
 \bigcirc 10^{-21}
 \bigcirc 10^{-24}
 \bullet 10^{-27}

FIG. 4. Sky map at the frequency of 1 GHz for a realization of clumps distribution. For each clump, the circle radius is proportional to the logarithm of radio flux.

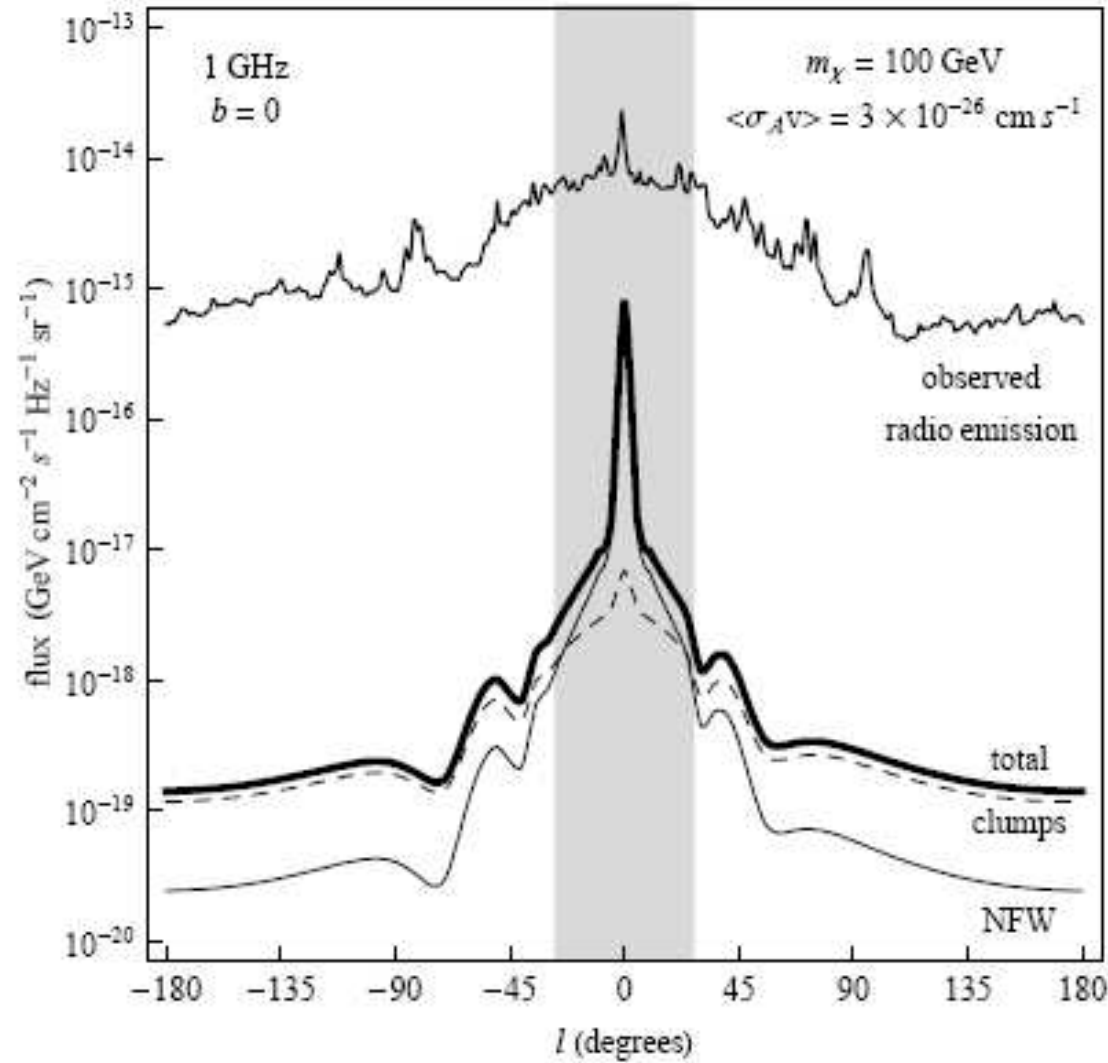
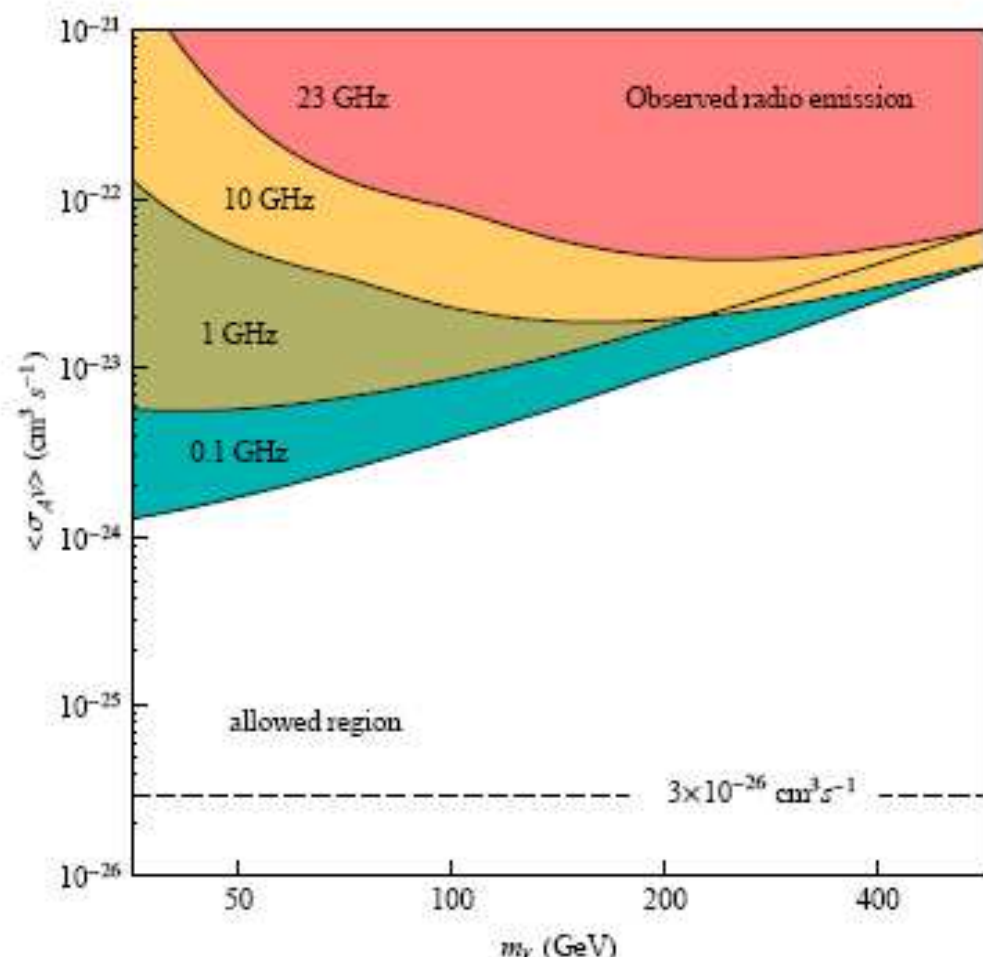


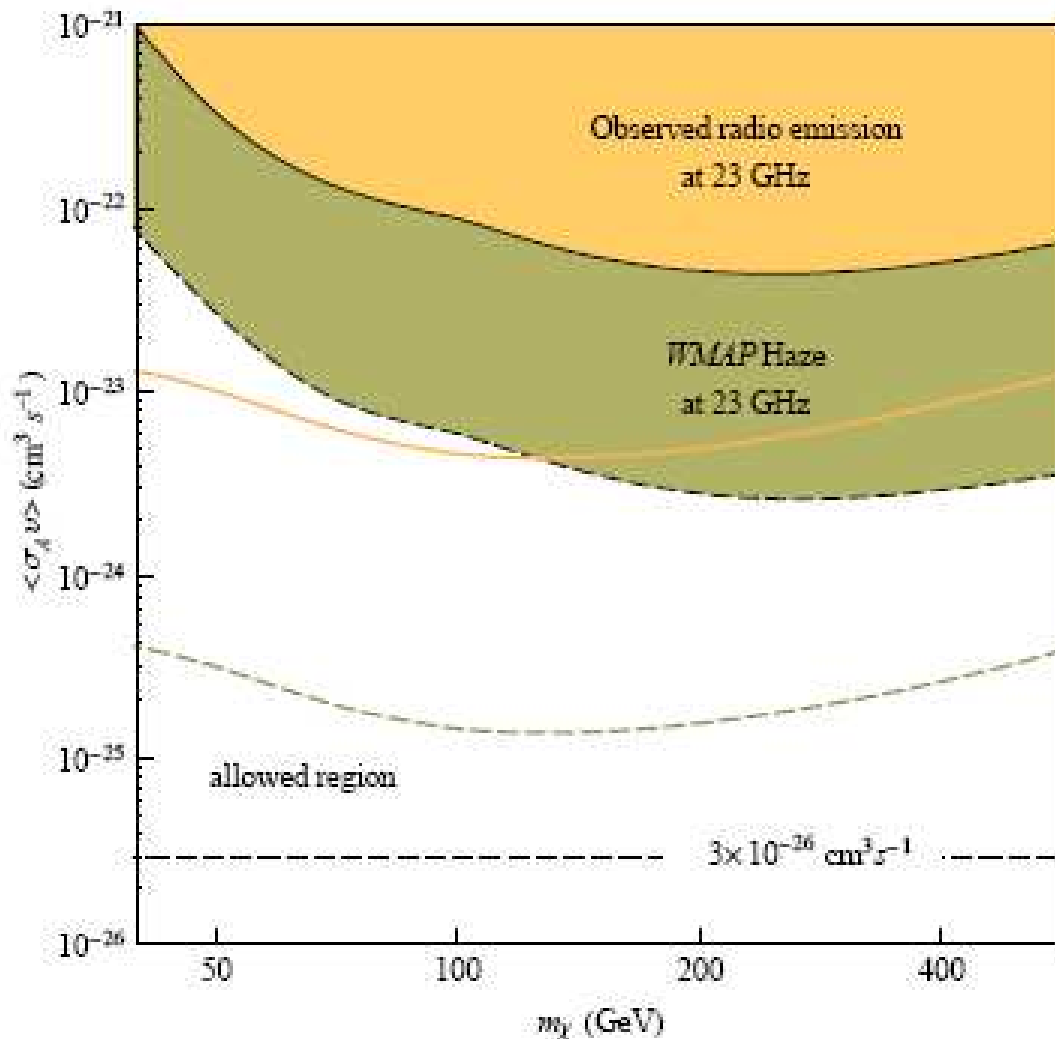
FIG. 6: DM synchrotron profile for the Halo and unresolved substructures and their sum at 1 GHz for $m_\chi = 100$ GeV and $\langle\sigma_A v\rangle = 3 \times 10^{-26} \text{ cm}^3 \text{ s}^{-1}$. The astrophysical observed emission at the same frequency is also shown.

DM ANNIHILATION CONSTRAINTS

In the analysis we use a small mask covering a $15^\circ \times 15^\circ$ region around the galactic center where other energy loss processes are at work



Exclusion plot in the m_χ - $\langle \sigma_A v \rangle$ plane. Assuming no dominant DM synchrotron emission. No foreground sub.



Exclusion plot in the $m_\chi - \langle \sigma_A v \rangle$ plane. Constraints from the WMAP 23 GHz foreground map and 23 GHz foreground cleaned residual map (the WMAP Haze) for the TT model of MF (filled regions) and for a uniform $10 \mu\text{G}$ field (dashed lines)

Results 1

- The use of the haze at 23 GHz gives about one order of magnitude better constraints with respect to the synchrotron foregrounds at the same frequency.
- The information at other frequencies are complementary giving better constraints at lower DM masses. The constraints improve of about one order of magnitude at $m_\chi = 100$ GeV from 23 GHz to 1 GHz while only a modest improvement is achieved considering further lower frequencies as 0.1 GHz.
- The DM signal has a broad frequency extent and also below 1 GHz is still relevant. This is a potential problem for the DM interpretation of the WMAP Haze. In the Haze extraction procedure, the observed radio emission at 408 MHz is used as template of the synchrotron background.

Constraints in the radio band are complementary to similar constraints in the X-ray/gamma band and from neutrinos.

Radio data, in particular, are more sensitive in the GeV–TeV region while neutrinos provide more stringent bounds for very high DM masses (≥ 10 TeV).

Gammas, instead, are more constraining for $m_\chi \leq 1$ GeV. The combination of the various observations provides thus interesting constraints over a wide range of masses pushing the allowed window significantly near the thermal relic possibility.

ICS signal in connection to Pamela

0903.1852 [astro-ph.GA]

In a WIMP scenario (a benchmark model): It would be favored a DM particle in the TeV range and with a thermally averaged annihilation cross section $\langle\sigma_A v\rangle \sim 10^{-23} \text{ cm}^3 \text{ s}^{-1}$

Atypical: i) $\langle\sigma_A v\rangle$ three orders of magnitude larger than values naturally expected.

ii) Hadronic channels mainly forbidden.

Suppressed hadronic channels imply only few (energetic) photons produced either if the annihilation takes place through the $\mu^+ \mu^-$ or $\tau^+ \tau^-$ channels or in the case of the $e^+ e^-$ channel through the presence of Final State Radiation.

However final leptons will produce e.m. signal via SR and ICS. We will focus on the signal coming from the Halo rather than from the GC

We calculate dN_e/dE with Dark-SUSY (Gondolo et al. 2004), which uses a tabulation of the spectrum of the decay products derived with Pythia (Sjostrand 2007).

His produces an almost constant spectrum with a cut off at the mass of the WIMP.

The electron source term for Galprop is then given by

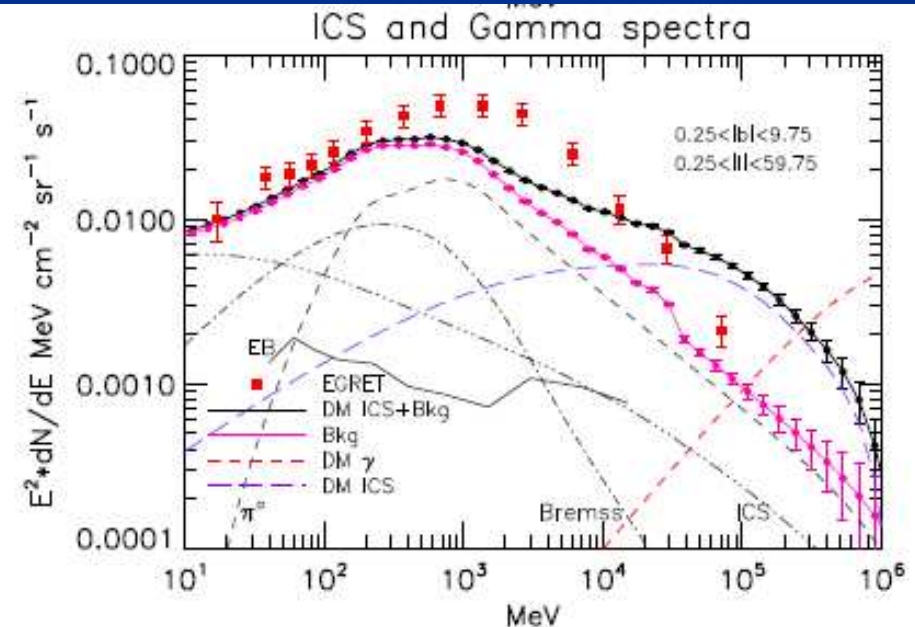
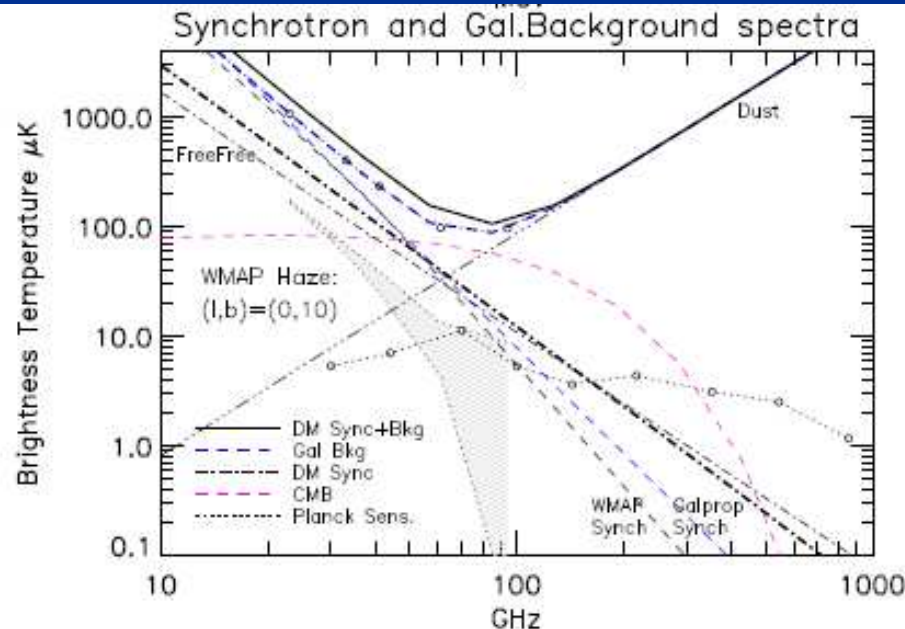
$$Q(r,E) = \rho^2 \langle \sigma_A v \rangle / 2m_\chi^2 dN_e/dE.$$

By using Galprop v50.1p to solve electron diffusion-loss equation.
We use for our calculation:

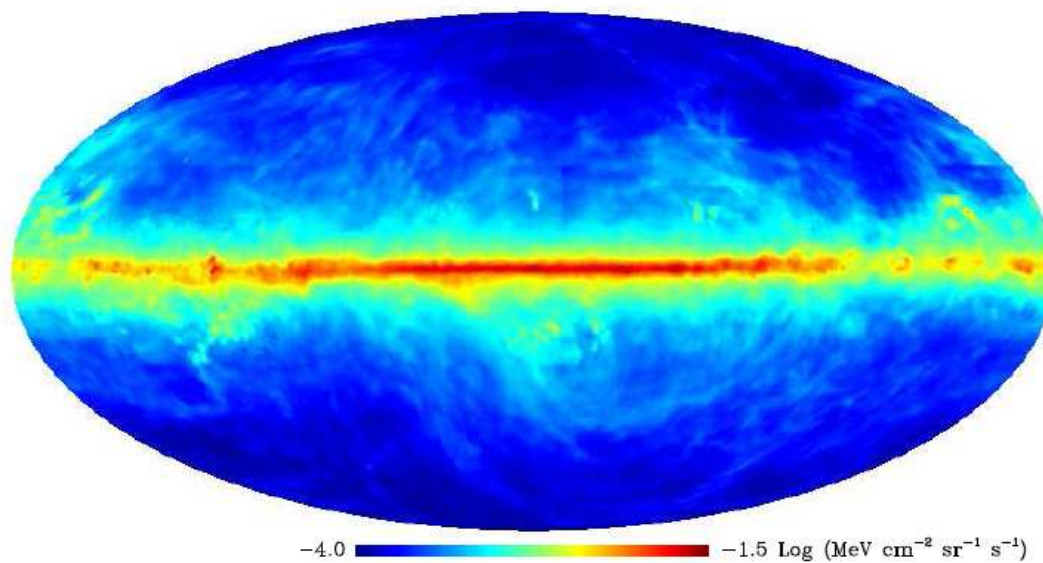
A diffusion coefficient $D = D_0 (E/E_0)^{-\alpha}$ with $D_0 = 5 \times 10^{28} \text{ cm}^2\text{s}^{-1}$, $E_0 = 3 \text{ GeV}$ and $\alpha = 0.33$, corresponding to a Kolmogorov spectrum of turbulence.

The transport eq. is solved in a cylinder of half-height $z = \pm 4 \text{ kpc}$ and radius $R = 20 \text{ kpc}$, while the GMF is modeled as $\langle B^2 \rangle^{1/2} = B_0 \exp(-r/r_B - |z|/z_B)$ with $B_0 = 11 \mu\text{G}$, $r_B = 10 \text{ kpc}$ and $z_B = 2 \text{ kpc}$.

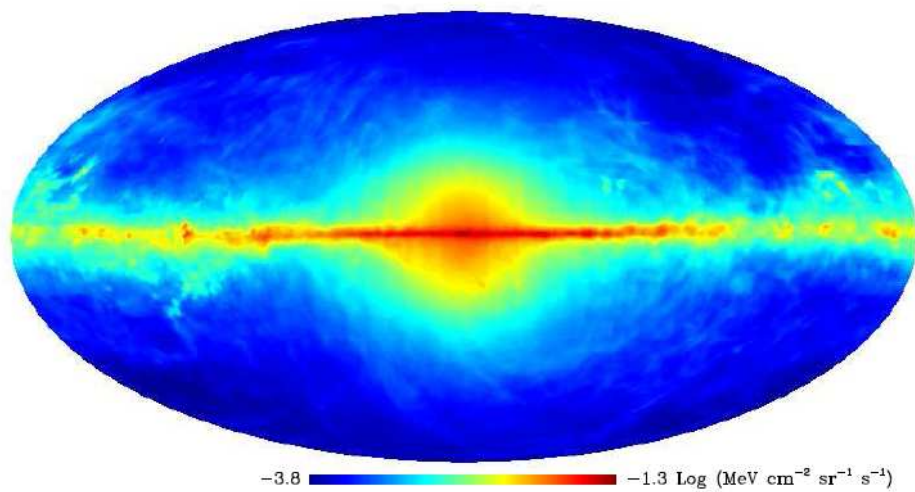
For DM we choose a very conservative isothermal cored profile



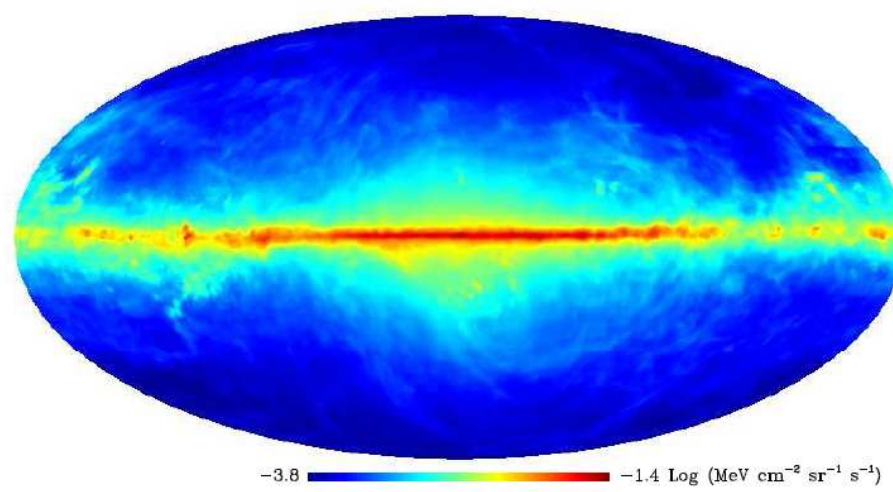
Gamma Sky at 10 GeV $E^2 \cdot dN/dE$



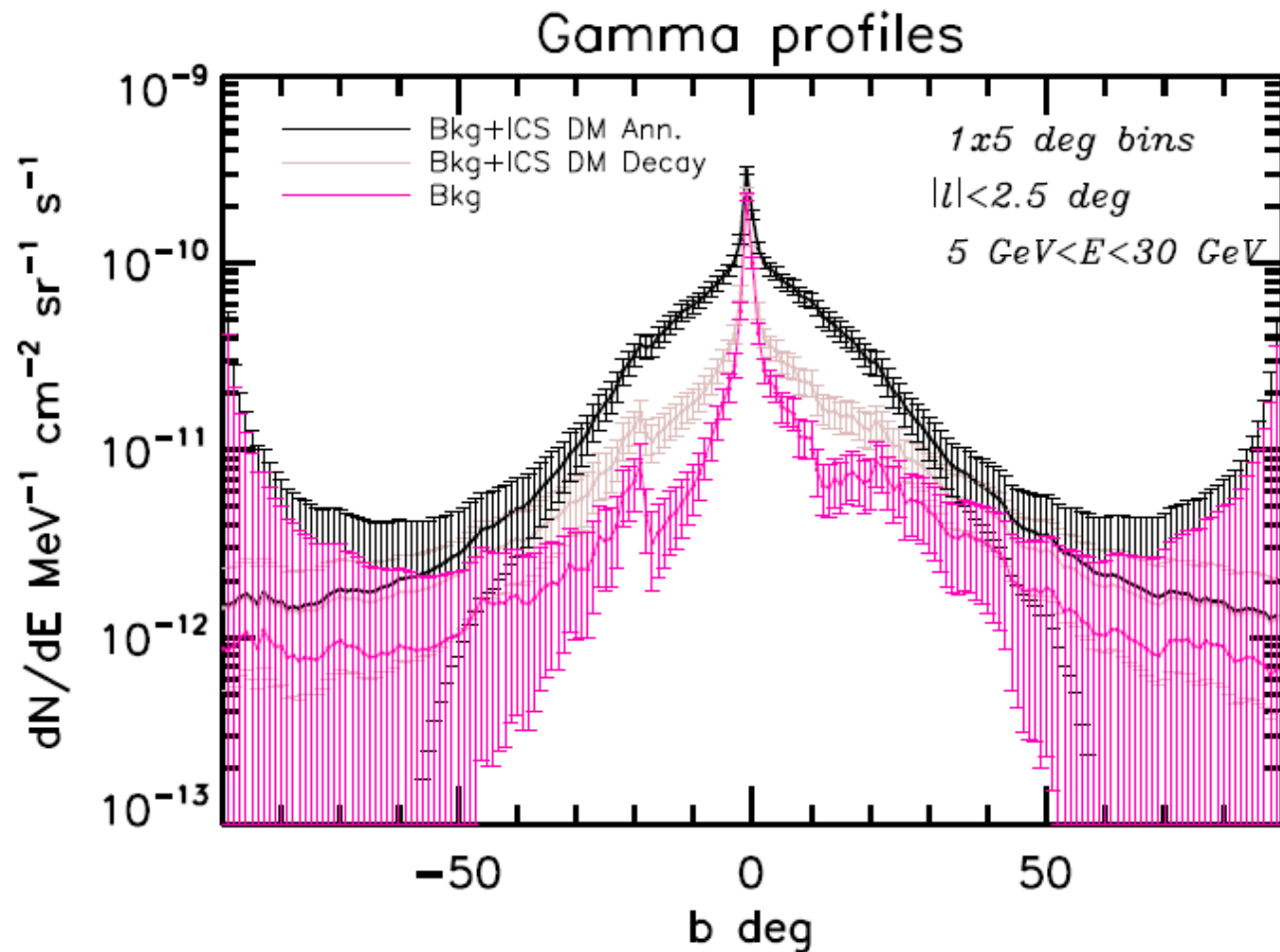
Gamma Sky Bkg + Dark Matter at 10 GeV $E^2 \cdot dN/dE$



Gamma Sky Bkg + Dark Matter at 10 GeV $E^2 \cdot dN/dE$



1. The errors expected with 1 y from Fermi are tiny enough to detect the excess with an high degree of CL.
2. The excess comes from the Halo, away from GC, thus less affected by uncertainties on DM profile and ISRF.
3. ICS excess has the shape of a circular Haze reflecting the DM distribution in the Halo. The CR background is expected to lie mostly along the galactic plane where the astrophysical sources are located.



The excellent Fermi ability to discriminate among the astrophysical and annihilating DM scenario. The analysis can be easily generalized to exploit the full angular shape of the IC Haze.

Results 2

- Fermi has the potential to test the DM interpretation of Pamela/ATIC results basically in a model independent way thanks to the strong IC signal expected.
- The IC signal would give rise to a striking “IC Haze” feature peaking around 10-100 GeV which would provide a further mean to discriminate the DM signal from the astrophysical backgrounds and/or to check for possible systematics.



Thank you for
listening!